Int. J. Heat Mass Transfer. Vol. 27, No. 9, pp. 1573–1582, 1984
Printed in Great Britain

0017–9310/84 $3.00 + 0.00

Vertical transient natural convection flows in cold water

YOGENDRA JOSHI and BENJAMIN GEBHART

Department of Mechanical Engineering and Applied Mechanics, University of Pennsylvania, Philadelphia, PA 19104, U.S.A.

(*Received* 11 *January* 1984)

Abstract—The initial, transient natural convection flow resulting from a sudden change of the boundary condition at a vertical surface has been examined. The ambient medium is cold water, giving rise to a density variation with temperature which may not be linearized. Closed-form solutions for flow velocity have been obtained from the known temperature solutions. Two important surface conditions have been considered. These are: (a) an initial step in the surface energy generation rate, both for zero and finite thermal capacity surfaces and, (b) a step in the surface temperature. Flow results have been computed for the entire range of ambient temperature conditions around that at the density extremum point. For suddenly heated surfaces, ambient temperatures larger than the extremum temperature result in upflow for all later times, although the velocities are much smaller than those obtained at higher temperature levels for identical heating conditions. For condition (a), ambient temperatures below the extremum result in a pure downflow for short times, followed by a bidirectional flow. For condition (b), by suitably transforming the velocity and distance variables, self-similar profiles are obtained. Conditions resulting in upflow, bidirectional flow and downflow are then examined. Dimensional comparisons of present results with those at higher ambient temperatures show the inapplicability of the Boussinesq formulation around the extremum point. In addition, it is shown necessary to use an accurate density equation by comparing the results with those using a parabolic density equation for water around 4°C.

INTRODUCTION

TRANSIENT natural convection flows arise in many kinds of processing and energy conversion equipment, including batch heating, equipment start-up and reactor reflooding. Their study began with Illingworth [1], who calculated the time evolution of the one-dimensional (1-D) flow adjacent to a doubly infinite vertical surface. Even for a surface with a leading edge, the initially 1-D transient conduction field causes buoyancy which initially also results in a 1-D velocity field. Later, such 1-D fields are supplanted by two-dimensional (2-D) time-evolving flow. This ultimately results in the well-known steady developing boundary layer flow, for unchanging surface input conditions. This sequence of events has been verified and studied in great detail, both analytically and experimentally, by numerous investigators. Many of these studies are summarized in Sammakia and Gebhart [2].

All of the studies referred to above are based on the Boussinesq linear approximation in the calculation of the buoyancy force in the fluid. However, this approximation is often not valid, for example, in cold water at temperatures near its density extremum. To treat these flows in a convenient and accurate manner, Gebhart and Mollendorf [3] developed a new equation of state for cold water, in the range $t = 0$–$20°C$, $s = 0$–40 ppt salinity and $p = 1$–1000 bar. This equation was used to analyze various flows in steady state [4].

Very few studies have been concerned with time-dependent non-Boussinesq flows. Cheng *et al.* [5] studied the transient natural convection cooling in a horizontal water pipe, with a convective boundary condition. The density of water was calculated using a four parameter equation of state. Numerical solutions have been presented both with and without supercooling of water. Vasseur and Robillard [6] considered the transient natural convection flow in a rectangular cavity filled with cold water. The water is assumed to be initially at a uniform temperature t_i. For time $\tau \geqslant 0$, the cavity walls are maintained at a temperature $t_0 = 0°C$. The resulting non-Boussinesq buoyancy force has been calculated using a fourth-order equation of state for cold water. The system of governing time-dependent partial differential equations was numerically solved for different aspect ratios and initial water temperatures varying between 4 and 21°C. The flow patterns and overall convective heat transfer were seen to be greatly influenced by the presence of the density extremum. The same geometry with convective wall conditions was considered by Robillard and Vasseur [7].

Pop and Raptis [8] recently examined the transient natural convection adjacent to a doubly infinite vertical surface, in water at 4°C, subject to a temperature step boundary condition. A second-order equation of state for cold water was used. By suitably transforming the distance and velocity variables, a set of self-similar equations was obtained. Solutions were presented both with and without blowing and suction at the surface. As discussed later, the analysis in ref. [8] with zero suction or blowing, is the special case of $R = 0$, for the more general formulation presented here.

This study deals with the transient 1-D natural

NOMENCLATURE

c'' thermal capacity of surface per unit area exposed to fluid
f nondimensional velocity function in ref. [8]
F $U/\bar{\tau}$
g acceleration due to gravity
k thermal conductivity of water
p pressure
Pr Prandtl number of water
q exponent in density equation (3)
q'' energy generation rate within the surface, per unit area
Q^* parameter associated with thermal capacity of surface in equation (14)
R parameter defined in equation (10)
R^* parameter defined in equation (9)
t local temperature of water, dimensional
T nondimensional local temperature in equations (9) and (10)
u dimensional velocity in the vertical direction
U nondimensional vertical velocity in equations (9) and (10)
v_0 blowing velocity at the surface in ref [8]
w thickness of Inconel 600 surface element
W buoyancy force, defined in equation (12)
x_p leading edge effect penetration distance
y dimensional horizontal coordinate
Y nondimensional horizontal coordinate in equations (9) and (10).

Greek symbols
α thermal diffusivity of water
$\hat{\alpha}$ parameter in the density equation (3)
β coefficient of thermal expansion of water, $-(\partial\rho/\partial t)_p/\rho$
η $Y/2(\bar{\tau}/Pr)^{1/2}$
ν kinematic viscosity of water
ξ $Y/2(\bar{\tau})^{1/2}$
ρ local density of water
τ dimensional time
$\bar{\tau}$ nondimensional time in equations (9) and (10).

Subscripts
f value at which fluid properties have been evaluated
i initial value
m value at the density extremum
r reference value
0 value at $y = 0$
∞ value in the ambient.

convection flow adjacent to a vertical surface, following an increase in the surface thermal condition, idealized as a step change. The transport is assumed to be 1-D, as early along a surface of limited height. The ambient water, assumed to be quiescent and unstratified, is at a temperature near the density extremum. Since the developing temperature and buoyancy force fields are 1-D, the momentum equation becomes linear.

A closed-form solution, for resulting flow velocity, in the form of a double integral, has been obtained using the method of Green's functions. Two important surface conditions have been considered, a step in surface heat flux and a step in surface temperature. Numerical computations of the temperature and resulting velocity fields have been carried out for $Pr = 11.6$, for the entire range of interest of the parameters, R and R^*, defined in equations (9) and (10) below.

ANALYSIS

The time-dependent 1-D flow adjacent to a vertical surface may be shown to be governed by the following set of equations in $u(y,\tau)$ and $t(y,\tau)$

$$\frac{\partial u}{\partial \tau} = \nu\frac{\partial^2 u}{\partial y^2} + \frac{g(\rho_\infty - \rho)}{\rho_r} \tag{1}$$

$$\frac{\partial t}{\partial \tau} = \alpha\frac{\partial^2 t}{\partial y^2}. \tag{2}$$

The following density equation of state has been developed by Gebhart and Mollendorf [3]

$$\rho(t) = \rho_m\{1 - \hat{\alpha}[|t - t_m|^q\}. \tag{3}$$

For pure water, at 1 bar, $\hat{\alpha} = 9.297173 \times 10^{-6}\ (°C)^{-q}$, $q = 1.894816$ and $t_m = 4.03°C$. Using equation (3) to calculate the buoyancy force, equation (1) is rewritten as

$$\frac{\partial u}{\partial \tau} = \nu\frac{\partial^2 u}{\partial y^2} + g\hat{\alpha}\{|t - t_m|^q - |t_\infty - t_m|^q\}. \tag{4}$$

The initial and remote conditions are

$$u(y,0) = t(y,0) - t_\infty = u(\infty,\tau) = 0. \tag{5}$$

The surface boundary conditions depend on the surface heating condition. The following two important circumstances are considered.

(a) Step increase in the surface element energy generation flux, from zero to a thereafter constant value q''. Then, for $\tau > 0$

$$c''\frac{\partial t}{\partial \tau}(0,\tau) - k\frac{\partial t}{\partial y}(0,\tau) = q'' \tag{6}$$

$$u(0,\tau) = 0 \tag{7}$$

where equation (6) is obtained through an energy balance on the surface element. For elements with negligible thermal capacity, c'', the first term in equation (6) vanishes.

(b) Step jump in the surface temperature; for $\tau > 0$

$$t(0,\tau) = t_0 \tag{8}$$

where equation (7) also applies.

The governing equations and boundary conditions are generalized for the flux and temperature step, conditions (a) and (b). The respective temperature quantities Δt and $(t_0 - t_\infty)$ and resulting characteristic velocities are used. For the input conditions (a) and (b), the resulting variables are

$$\text{(a)}\quad U = \frac{u}{[g\hat{\alpha}\nu^{(q+1)}q''^q/k^q]^{1/(q+3)}};$$

$$T = \frac{(t-t_\infty)}{\Delta t} = \frac{(t-t_\infty)}{[\nu^2 q''^3/g\hat{\alpha}k^3]^{1/(q+3)}}$$

$$\bar{\tau} = \frac{\tau}{[k^{q\nu(1-q)/2}/g\hat{\alpha}q''^q]^{2/(q+3)}};$$

$$Y = \frac{y}{[\nu^2 k^q/g\hat{\alpha}q''^q]^{1/(q+3)}}$$

and

$$R^* = \frac{(t_m - t_\infty)}{\Delta t} = \frac{t_m - t_\infty}{[\nu^2 q''^3/g\hat{\alpha}k^3]^{1/(q+3)}}. \tag{9}$$

$$\text{(b)}\quad U = \frac{u}{[g\hat{\alpha}\nu(t_0-t_\infty)^q]^{1/3}}, \quad T = \frac{(t-t_\infty)}{(t_0-t_\infty)}$$

$$\bar{\tau} = \frac{\tau}{[\nu^{1/2}/g\hat{\alpha}(t_0-t_\infty)^q]^{2/3}},$$

$$Y = \frac{y}{[\nu^2/g\hat{\alpha}(t_0-t_\infty)^q]^{1/3}}$$

and

$$R = \frac{(t_m - t_\infty)}{(t_0 - t_\infty)}. \tag{10}$$

For both the q'' and t_0 surface conditions, conditions (a) and (b), equations (2) and (4) transform to

$$\frac{\partial T}{\partial \bar{\tau}} = \frac{1}{Pr}\frac{\partial^2 T}{\partial Y^2} \tag{11}$$

$$\frac{\partial U}{\partial \bar{\tau}} = \frac{\partial^2 U}{\partial Y^2} + \{|T - R^*|^q - |R^*|^q\}$$

$$= \partial^2 U/\partial Y^2 + W(Y,\bar{\tau}) \tag{12}$$

where W is the buoyancy force and R^* in equation (12) becomes R for the temperature step condition. The initial and boundary conditions for the flux input condition are

$$U(Y,0) = T(Y,0) = U(0,\bar{\tau}) = U(\infty,\bar{\tau}) = T(\infty,\bar{\tau}) = 0 \tag{13}$$

$$Q^* \frac{\partial T(0,\bar{\tau})}{\partial \bar{\tau}} - \frac{\partial T(0,\bar{\tau})}{\partial Y} = 1 \tag{14a}$$

where

$$Q^* = c''\left[\frac{g\hat{\alpha}q''^q\nu^{(q+1)}}{k^{(2q+3)}}\right]^{(1/q+3)}. \tag{14b}$$

Here, Q^* is the nondimensional parameter associated with the relative thermal capacity of the surface. For the temperature step, the conditions given in equation (13) again apply. However, the condition at the surface, for $\bar{\tau} \geqslant 0$, is now

$$T(0,\bar{\tau}) = 1. \tag{15}$$

Since equation (11) is for 1-D transient conduction, solutions are readily available for both surface step conditions; see, for example, Goldstein and Briggs [9]. For a step in energy generation rate

$$T(Y,\bar{\tau}) = \frac{Q^*}{Pr}\left[\frac{2}{Q^*}\left(\frac{\bar{\tau}\,Pr}{\pi}\right)^{1/2} e^{-\eta^2} - \frac{2}{Q^*}(\bar{\tau}\,Pr)^{1/2}\eta\ \text{erfc}\,\eta + \text{erfc}\left\{\eta + \frac{(Pr\,\bar{\tau})^{1/2}}{Q^*}\right\}\exp\left\{\frac{2(Pr\,\bar{\tau})^{1/2}}{Q^*}\eta + \frac{\bar{\tau}\,Pr}{Q^{*2}}\right\} - \text{erfc}\,\eta\right] \tag{16}$$

where

$$\eta = \frac{Y}{2(\bar{\tau}/Pr)^{1/2}}.$$

For $Q^* = 0$ this simplifies to

$$T(Y,\bar{\tau}) = 2(\bar{\tau}/Pr)^{1/2}\ \text{i erfc}\,\eta. \tag{17}$$

For the temperature step the solution is

$$T(Y,\bar{\tau}) = \text{erfc}\,\eta \tag{18}$$

where η is the same as in equation (16) with Y and $\bar{\tau}$ defined in equation (10).

The momentum equation, equation (12), is 1-D with a space- and time-dependent source term, the buoyancy. Solutions were constructed from equation (12), using Green's functions. For the flux surface condition the solution is

$$U(Y,\bar{\tau}) = \int_{\xi=0}^{\bar{\tau}} d\xi \int_{y'=0}^{\infty} [4\pi(\bar{\tau}-\xi)]^{-1/2} \times \left[\exp\left\{-\frac{(Y-y')^2}{4(\bar{\tau}-\xi)}\right\} - \exp\left\{-\frac{(Y+y')^2}{4(\bar{\tau}-\xi)}\right\}\right] \times \{|T-R^*|^q - |R^*|^q\}\,dy'. \tag{19}$$

For the temperature step condition, equation (18) is used in equation (12). The solution is again equation (19) above, where R^* is replaced by R.

Equation (19) was numerically integrated, using Simpson's rule. In evaluating the inner integral, the upper limit on y' was taken to be $4\sqrt{(4\bar{\tau}/Pr)}$. In addition $\Delta y' = 0.08\sqrt{(4\bar{\tau}/Pr)}$ and $\Delta\xi = \bar{\tau}/600$ were used.

RESULTS

All computations were carried out for pure water at 1 bar pressure. A Prandtl number value of 11.6 was used. The parameters R^* and R characterize the buoyancy force, W, and, therefore the flow condition. Over the whole ranges of variation of R^* and R, the buoyancy force distributions change and both bidirectional

Table 1. Summary of flow directions for various R^* for the energy step input

$R^* \leqslant 0$	$R^* > 0$
Upflow for all times	Downflow initially. Bidirectional flow for large times

buoyancy and flows arise. Tables 1 and 2 summarize these mechanisms, in terms of the ranges of R^* and R, wherein they arise.

The detailed transport characteristics for the two surface temperature conditions are presented in Figs. 2–9. The flux input condition is considered first, for the simplest circumstance of $Q^* = 0$. Finite values of Q^* have significant effects on the transport, which are discussed subsequently. Finally, the temperature step condition is shown to result in self-similar solutions for all R. The implications of self similarity are discussed in detail.

A flux input to a surface of negligible thermal capacity, that is $Q^* = 0$

As shown in Table 1, any value of $R^* > 0$, for which $t_m > t_\infty$, results in an initial downflow, later supplanted by a bidirectional flow. A representative value of $R^* = 0.2$ is chosen in the following to illustrate the important features of such flows. Taking $t_\infty = 3.5°C$ results in $q'' = 861.5$ W m^{-2} for $R^* = 0.2$, when fluid properties are taken at 4.44°C in equation (9). This value of q'' is a common level in actual circumstances. The resulting buoyancy and velocity responses, for $R^* = 0.2$, are shown in Figs. 2 and 3.

The variation of the buoyancy force, $W(Y, \bar{\tau})$ in equation (12), with time, for $R^* > 0$, that is, $t_m > t_\infty$, can be qualitatively understood by considering Fig. 1. With the sudden step in energy generation within the surface, the surface temperature t_0 begins to increase above t_∞. The resulting buoyancy force at the surface and out across the heated fluid layer remains downward until the surface temperature t_0 increases to beyond t_2 in Fig. 1. Thereafter, the buoyancy force is upward at the surface and near it. Then W is bidirectional; upward near the surface and downward further out.

Distributions of W are plotted, for $R^* = 0.2$, in Fig. 2, at various times $\bar{\tau} = 1, \ldots, 11$. For $\bar{\tau} = 1$, the buoyancy force is downward across the entire thermal layer. However, by $\bar{\tau} = 2$, the surface temperature t_0 has already risen above, say t_2 on Fig. 1, and the buoyancy force is bidirectional with a thin region of upward buoyancy near the surface. At later times the upward

Table 2. Summary of flow directions for various R for surface temperature step input

$-\infty < R \leqslant 0$	$0 < R < 0.31$	$0.31 \leqslant R \leqslant \infty$
Upflow for all times	Bidirectional flow for all times	Downflow for all times

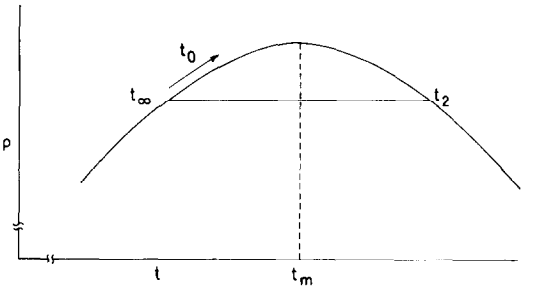

FIG. 1. Density variation of cold water showing the qualitative temperature response of a surface following a step input in the surface energy generation rate.

buoyancy force becomes bigger near the surface and positive buoyancy penetrates further out into the thermal layer.

The velocity distributions resulting from this changing buoyancy force distribution are shown in Fig. 3. Since buoyancy is the only driving force, the flow in Fig. 3 follows directly from the W distribution in Fig. 2. However, the effects of inertia and viscosity in equation (12) result in a delay in the time response of the velocity profile. Although the buoyancy force has already become bidirectional at $\bar{\tau} = 2$, the flow is completely downflow, even up to $\bar{\tau} = 5$.

The time variation of the buoyancy force at the surface, $W(0, \bar{\tau})$, is plotted in Fig. 4, for various values of the input parameter R^*. For $R^* \leqslant 0$, as for q'' positive and $t_\infty > t_m$, increasing t_0 above t_∞ always results in only increasing upward buoyancy. For any $R^* > 0$, as for $t_\infty < t_m$, $W(0, \bar{\tau})$ has a minimum value as t_0 reaches t_m. Then it increases till eventually it becomes positive. The further role of R^*, in drastically increasing the time for which complete downflow will persist, is clear by comparing the curves for $R^* = 0.2$ and 0.5.

A surface element of appreciable thermal capacity, that is $Q^* \geq 0$

The characteristic parameter Q^* is given in equation (14b). Values of Q^* for various input flux levels q'' and surface element thickness, w, for Inconel 600, are collected in Table 3. Water properties in Q^* have been evaluated at 4.44°C. As in equation (14b), Q^* increases with both q'' and w. For $w = 0.0762$ and 0.254 mm (3 and 10 mil), Q^* ranges between about 0.4 and 2 for q'' in the range 500–2000 W m^{-2}. Such values of w and q'' are typical of experiments. In Fig. 5, the salient features of transient response for $Q^* = 1.5$ are presented for $R^* = 0.2$.

Table 3. Computed values of Q^* for various q''(W m^{-2}) and surface thicknesses w(10^{-3} m) of Inconel 600

	q''(W m^{-2})			
w(10^{-3} m)	500	1000	1500	2000
0.0762	0.385	0.504	0.589	0.659
0.2540	1.284	1.679	1.964	2.196
0.7620	3.852	5.037	5.893	6.588
2.540	12.839	16.791	19.644	21.958

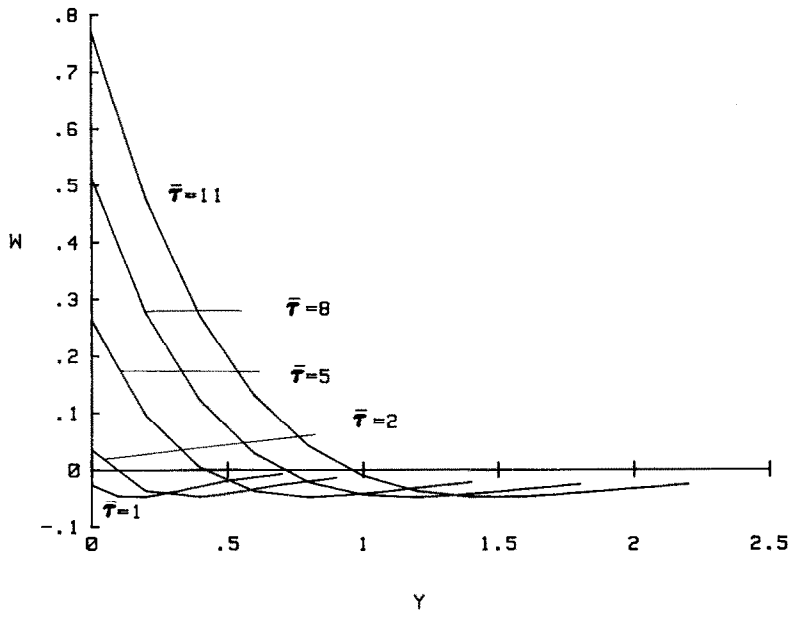

FIG. 2. Buoyancy force distribution at various time levels for a step input in the surface energy generation rate, for $Q^* = 0$ and $R^* = 0.2$.

Comparing these responses with those in Fig. 3 for $Q^* = 0$ indicates that thermal capacity delays response and the onset of buoyancy force reversal, that is of $W(0, \bar{\tau})$ becoming positive as t_0 exceeds t_2. The fluid temperatures do not rise as quickly and t_0 is delayed in reaching t_2. This results in the generation of a much stronger early downflow. Maximum downward velocity continues to increase until $\bar{\tau} = 14$, whereas in Fig. 3, it starts to decrease beyond $\bar{\tau} = 11$. The maximum upward velocity level at a given time is also less. These effects follow from the smaller upward buoyancy force due to the absorption of part of q'' by the surface material.

Next we consider the transient responses for $t_\infty > t_m$, when $q'' > 0$. The result is upflow for all times, as for flows at yet higher ambient temperatures, for which the Boussinesq approximation may be applicable. However, the nonlinearity of the temperature–density variation of water at low temperature levels results in much weaker buoyancy forces. These flows are

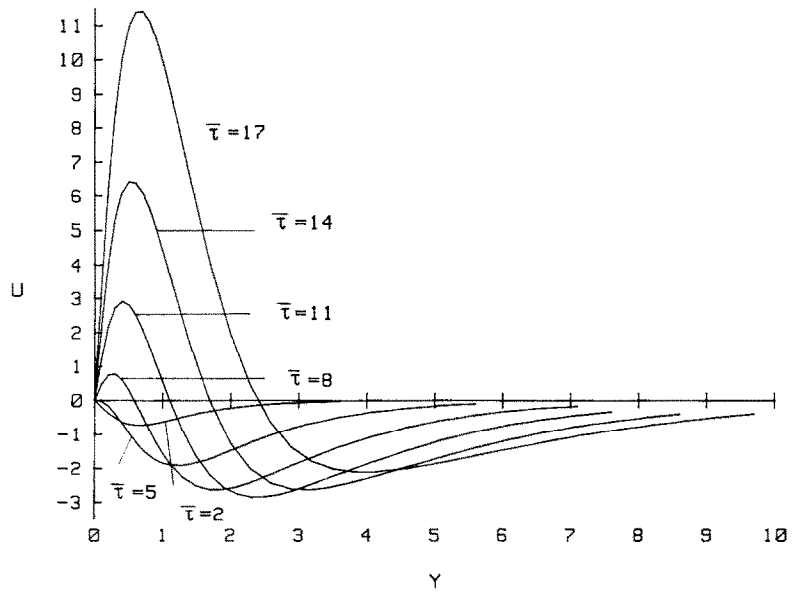

FIG. 3. Resulting velocity profiles at various time levels for $Q^* = 0$ and $R^* = 0.2$ for a step input in the surface energy generation rate.

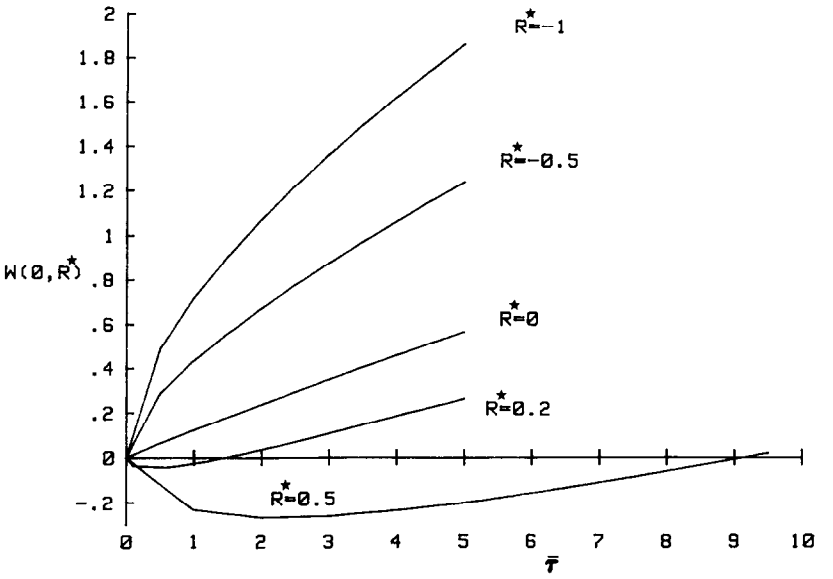

FIG. 4. Surface buoyancy force $W(0, R^*)$ variation with time, for a step input in the surface energy generation rate, for $Q^* = 0$.

therefore expected to be slower than those at higher ambient temperatures, for the same heating condition, q''.

Figure 6 shows an example of this effect for $q'' = 500\ \text{W m}^{-2}$ at $\tau = 46.5$ s. Water properties correspond to the indicated values of the temperature-dependent Prandtl number. The Boussinesq solution, at $Pr = 9.4$ that is for $t_f = 10.0°\text{C}$, yields the highest velocities. For the Boussinesq solution at $Pr = 11.35$, or $t_f = 4.4°\text{C}$, the coefficient of thermal expansion of water, β, is much smaller in magnitude and hence the velocities are lower than for $Pr = 9.4$. The accurate cold water calculations for $Pr = 11.6$, for $t_f = 4.0°\text{C}$, result in very much lower velocity levels than either of the two Boussinesq solutions. This clearly indicates the inapplicability of the Boussinesq approximation near the density extremum.

Transient following a sudden increase of surface temperature from t_∞ to t_0

The equations are (11) and (12), with R^* replaced by R. The boundary conditions indicate that the velocity and temperature profiles are self-similar under the transformation $\xi = Y/2\sqrt{\bar{\tau}}$ and $F(\xi) = (U/\bar{\tau})$,

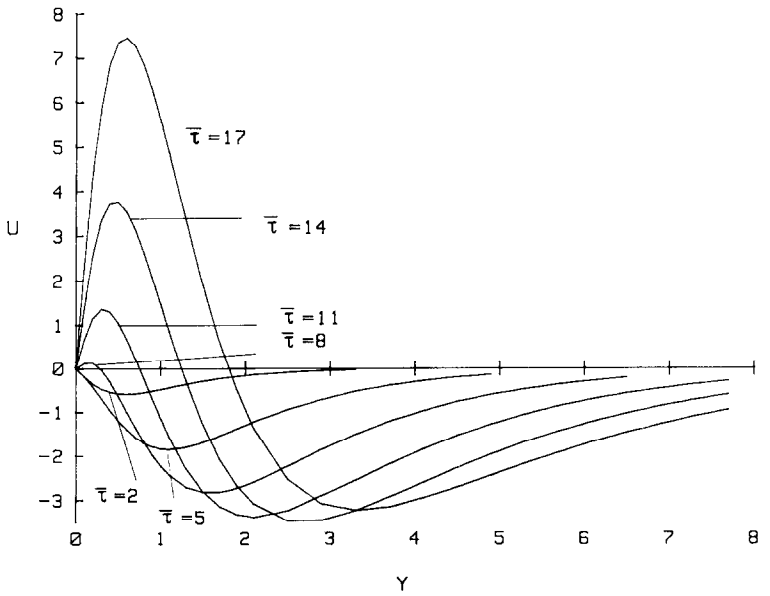

FIG. 5. Velocity profiles at various times after a step input in the surface energy generation rate for a surface with finite thermal capacity. $Q^* = 1.5$, $R^* = 0.2$.

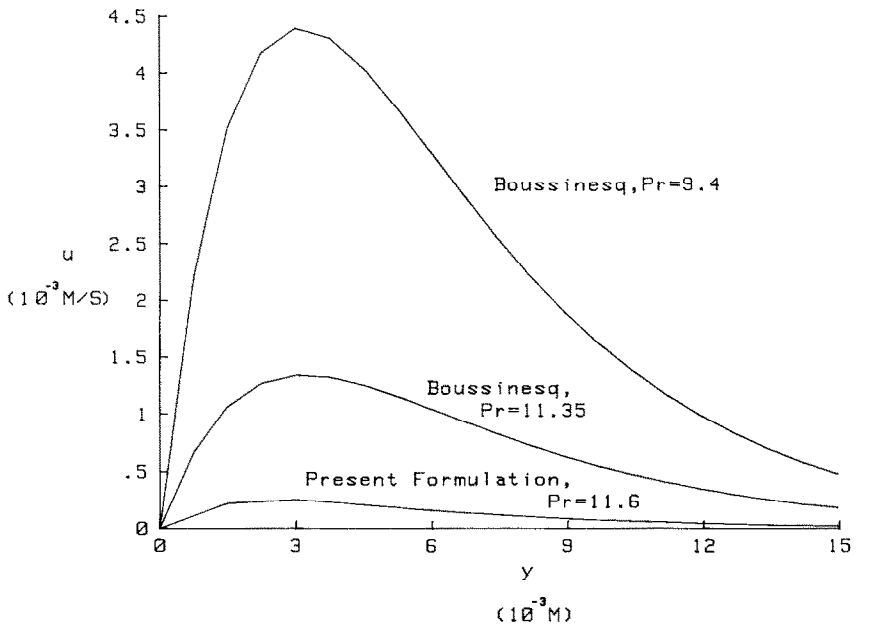

FIG. 6. Comparison of dimensional velocity profiles resulting from $q'' = 500$ W m^{-2}, $Q^* = 0$ and $\tau = 46.5$ s. Fluid properties have been evaluated at the indicated Prandtl number.

for any values of R and Pr. The governing equation for the velocity $F(\xi, R, Pr)$, in terms of $T(\xi, Pr)$ becomes

$$F''-4F+2\xi F'+4\{|T-R|^q-|R|^q\}=0 \qquad (20)$$

where R is defined in equation (10) and T and the boundary condition are

$$T = \text{erfc}\,(\xi\sqrt{Pr}) \qquad (21)$$

$$F(0, R, Pr) = F(\infty, R, Pr) = 0. \qquad (22)$$

Pop and Raptis [8] calculated such a transient natural convection response for a step increase in surface temperature in water at 4°C. This amounts here to the special example $R = 0$. The effect of suction or blowing at the plate was included and an additional parameter $c = -v_0(\bar{\tau}/\nu)^{1/2}$ arose. The density variation of water was assumed as a parabolic function of temperature, that is, $q = 2$. Thus for $c = 0$, the results in ref. [8] are for $R = 0$ and $q = 2$ in the present formulation.

The effects of R on flow again result from the buoyancy force distribution $W(\xi, R, Pr)$ as plotted in Fig. 7 in the range $-0.2 \leqslant R \leqslant 0.5$. For $R \leqslant 0$, W is positive across the whole heated layer. The maximum temperature in the flow region occurs at the surface and hence the buoyancy force is always the greatest there. The surface value of the buoyancy force is given by

$$W(0, R, Pr) = |1-R|^q-|R|^q. \qquad (23)$$

The necessary condition for $W(0, R, Pr) \leqslant 0$ is $R \leqslant 1/2$. Hence for $R \geqslant 1/2$, the buoyancy force is downward everywhere. A bidirectional buoyancy force distribution is seen in the intermediate range of $0 < R < 1/2$. It is upward near the surface and downward near the outer edge.

The resulting velocity $F(\xi, R, Pr)$ in the range $-0.2 \leqslant R \leqslant 0.5$ is obtained through the solution of equation (20) with $q = 1.894816$, subject to the boundary conditions in equation (22). A numerical shooting technique was used. Figure 8 shows $F(\xi)$ across the flow layer, for various R. For $-0.2 \leqslant R \leqslant 0$, which results for a heated surface when $t_\infty > t_m$, upflow was found over the whole region. This is in accordance with Fig. 7 where $W \geqslant 0$ for $-0.2 \leqslant R \leqslant 0$. In the range $0 < R < 1/2$ the distribution of W in Fig. 7 is bidirectional. However, the velocity $F(\xi, R, Pr)$ in Fig. 8 becomes completely downward for all ξ, for R of approximately 0.31 or larger. This is due to the combined effects of viscosity and inertia. Thus for $0.31 < R < 1/2$, even though the buoyancy force is upward near the surface, the flow is purely downward for all ξ.

The self-similar behavior of $(U/\bar{\tau})$ of these flows imparts a unique character to them. Flow is either unidirectional or bidirectional for all times. Which characteristic arises depends on the particular value of R. These flow responses are in contrast to those in Fig. 3. There the increasing surface temperature first results in a totally downward flow. Later a bidirectional flow arises. Since a self-similar solution is not found for the flux step input, velocity profiles change shape with time.

The present results for $R = 0$ using a more accurate equation of state have been compared with those of Pop and Raptis [8]. The ratio of (u/τ) from the present results for $R = 0$, to those in ref. [8] for no suction or blowing, is given by

$$\frac{(u/\tau)_{\text{present}}}{(u/\tau)_{\text{ref. [8]}}} = (t_0-t_\infty)^{(2-q)}\left(\frac{\kappa f(\xi)}{\hat{\alpha}F(\xi)}\right) \qquad (24)$$

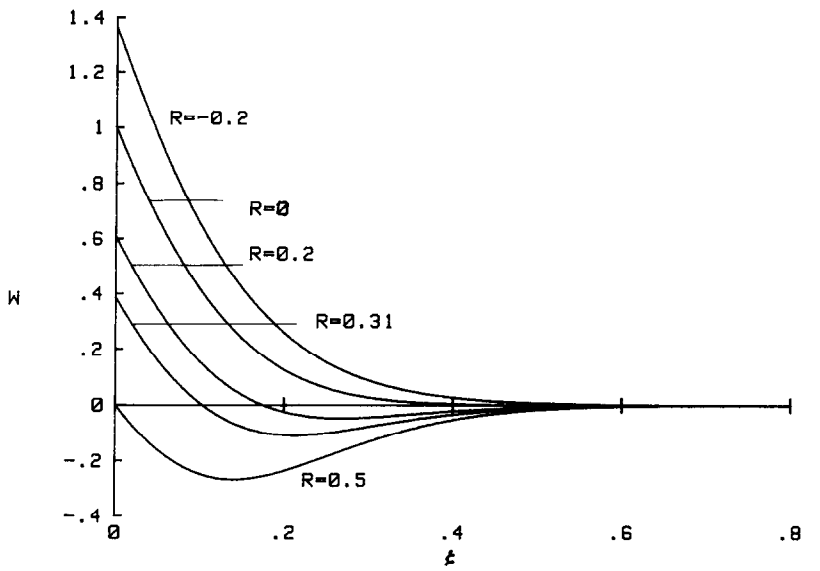

FIG. 7. Buoyancy force distribution $W(\xi, R)$ resulting from a step increase in surface temperature.

where $f(\xi)$ is the nondimensional velocity function and $\kappa = 8 \times 10^{-6}(°C)^{-2}$ from ref. [8].

Equation (24) has been plotted as a function of ξ for $Pr = 11.35$ in Fig. 9. The results from ref. [8] are seen to fall below the present results for $(t_0 - t_\infty) = 1°C$, the error increasing for large ξ. For $(t_0 - t_\infty) = 6°C$, the two analyses are seen to be in close agreement for small ξ but for large ξ, the error is again significant. For $(t_0 - t_\infty) = 8°C$, the analysis in ref. [8] gives higher values for small ξ and lower values for large ξ, when compared to the present results. It seems clear from this comparison that an accurate equation of state is necessary to get reliable quantitative results near the density extremum.

Leading edge effect propagation

The time interval during which the foregoing 1-D solutions are valid downstream of a leading edge is an important consideration. For flows wherein the Boussinesq approximation applies, a 'leading-edge effect' propagation distance was postulated by Goldstein and Briggs [9] as

$$x_p(\tau) = \max\left[\int_0^\tau u(y, t')\, dt'\right] \tag{25}$$

where the maximization in equation (25) is carried over y.

Experimental observations of Gebhart and Dring [10] and Mahajan and Gebhart [11] have shown,

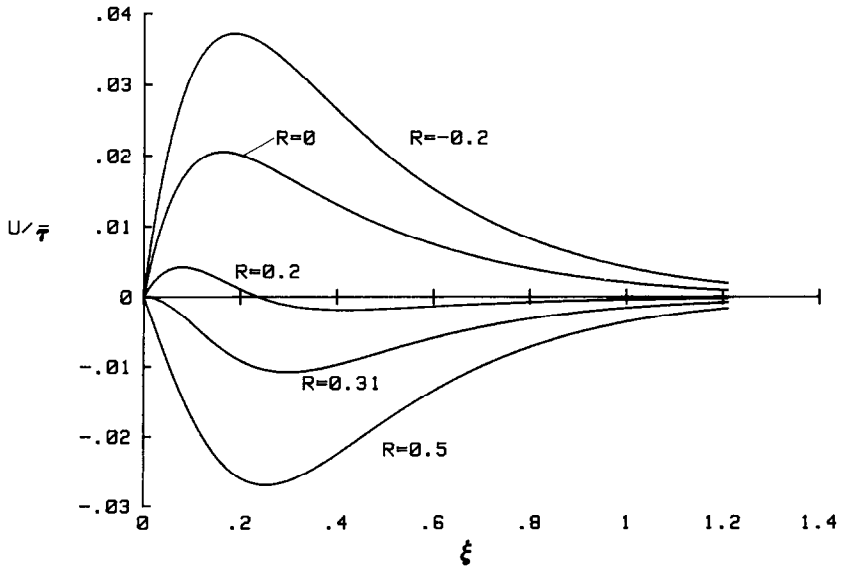

FIG. 8. Normalized velocity profiles $F(\xi, R)$ resulting from a step increase in surface temperature.

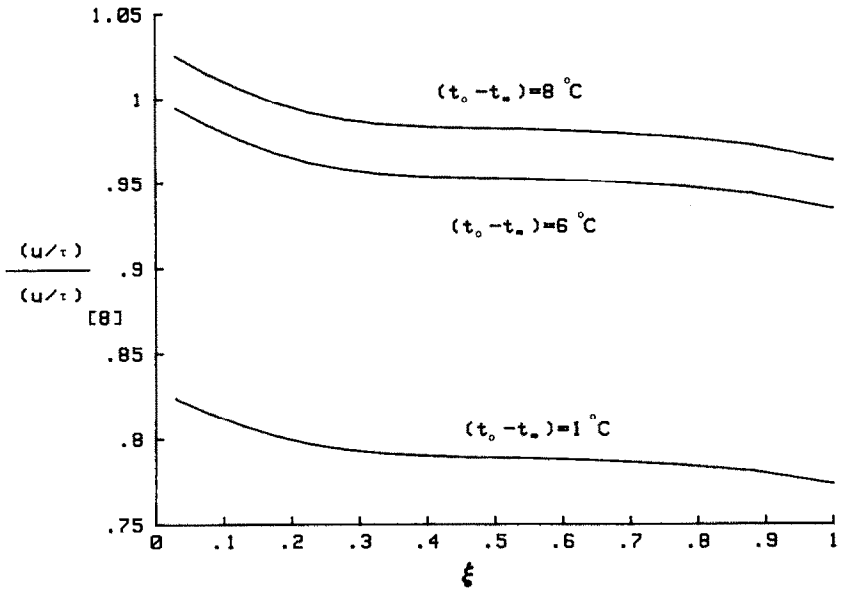

FIG. 9. Comparison of the velocity response from present analysis for a step increase in surface temperature with that of Pop and Raptis [8] for $R = 0$.

however, that for step input of surface energy generation rate, the 'leading-edge effect' actually propagates about twice as fast as indicated by calculations in ref. [9]. The reason for this difference is still not clearly understood.

Brown and Riley [12] questioned the method in ref. [9]. Their argument that the fastest leading edge signal travels at the maximum velocity in the boundary layer leads to a slightly faster propagation distance given by

$$x_p(\tau) = \int_0^\tau \max\,[u(y,t')]\,dt' \qquad (26)$$

where the maximization is again carried over y. The propagation calculations in ref. [8] are also based on the method in ref. [9].

For the non-Boussinesq behavior considered here, a similarly simple analytical expression for 'leading-edge effect' propagation does not appear feasible. Also, with bidirectional flow, there will also be a 'trailing-edge effect'. Thereby, the interval of validity of the 1-D solutions will be further modified. Such flows must be studied experimentally to determine any interval in which such solutions are applicable.

Acknowledgements—Many helpful discussions with Dr B. Sammakia are acknowledged. This study was carried out under National Science Foundation grant MEA 8200613. The manuscript was typed by Ms Anita Jackson.

REFERENCES

1. C. R. Illingworth, Unsteady laminar flow of gas near an infinite plate, *Proc. Camb. Phil. Soc.* **46** (4), 603–613 (1950).
2. B. Sammakia and B. Gebhart, Measurements and calculations of transient natural convection in water, *Trans. Am. Soc. Mech. Engrs*, Series C, *J. Heat Transfer* **104**, 644–648 (1982).
3. B. Gebhart and J. C. Mollendorf, A new density relation for pure and saline water, *Deep-Sea Res.* **24**, 831–848 (1977).
4. B. Gebhart and J. C. Mollendorf, Buoyancy induced flows in water under conditions in which density extrema may arise, *J. Fluid Mech.* **89** (4), 673–707 (1978).
5. K. C. Cheng, M. Takeuchi and R. R. Gilpin, Transient natural convection in horizontal water pipes with maximum density effect and supercooling, *Num. Heat Transfer* **1**, 101–115 (1978).
6. P. Vasseur and L. Robillard, Transient natural convection heat transfer in a mass of water cooled through 4°C, *Int. J. Heat Mass Transfer* **23**, 1195–1205 (1980).
7. L. Robillard and P. Vasseur, Transient natural convection heat transfer of water with maximum density effect and supercooling, *Trans. Am. Soc. Mech. Engrs*, Series C, *J. Heat Transfer* **103**, 528–534 (1981).
8. I. Pop and A. Raptis, A note on transient free convection of water at 4°C over a doubly infinite vertical porous plate, *Trans. Am. Soc. Mech. Engrs*, Series C, *J. Heat Transfer* **104**, 800–802 (1982).
9. R. J. Goldstein and D. G. Briggs, Transient free convection about vertical plates and cylinders, *Trans. Am. Soc. Mech. Engrs*, Series C, *J. Heat Transfer* **86**, 490 (1964).
10. B. Gebhart and R. P. Dring, The leading edge effect in transient natural convection flow from a vertical plate, *Trans. Am. Soc. Mech. Engrs*, Series C, *J. Heat Transfer* **89**, 24 (1967).
11. R. L. Mahajan and B. Gebhart, Leading edge effects in transient natural convection flow adjacent to a vertical surface, *Trans. Am. Soc. Mech. Engrs*, Series C, *J. Heat Transfer* **100**, 731–733 (1978).
12. S. N. Brown and N. Riley, Flow past a suddenly heated vertical plate, *J. Fluid Mech.* **59**, 225–237 (1973).

DES ECOULEMENTS VERTICAUX VARIABLES DE CONVECTION NATURELLE DANS L'EAU FROIDE

Résumé—On examine l'écoulement initial transitoire de convection naturelle qui résulte d'un changement soudain de condition aux limites sur une surface verticale. Le milieu ambiant est de l'eau froide, dont la densité augmentant avec la température ne peut être linéarisée. Des solutions analytiques pour la vitesse sont obtenues à partir des solutions connues de température. Deux conditions de surface sont considérées: (a) un échelon initial de flux à la surface, à la fois pour une capacité thermique de la surface nulle et finie et (b) un échelon de température de la surface. Les résultats sont calculés pour le domaine entier des conditions de température ambiante autour du point d'extrémum de densité. Pour des surfaces chauffées brusquement, des températures ambiantes plus grandes que la température extrémale apparaissent dans l'écoulement ascendant pour tous les temps ultérieurs, bien que les vitesses soient plus faibles que celles obtenues pour des niveaux de température plus élevés pour des conditions de chauffage identique. Pour la condition (a), des températures ambiantes inférieures à l'extremum apparaissent dans un écoulement descendant pendant un temps court et elles sont suivies par un écoulement bidirectionnel. Pour la condition (b), on obtient des profils self similaires par une transformation convenable des variables vitesse et distance. On examine les conditions d'un mouvement ascendant bidirectionnel et descendant. Des comparaisons dimensionnelles des résultats presents avec ceux à des températures ambiantes plus élevées montrent l'inapplicabilité de l'hypothèse de Boussinesq autour du point d'extremum. De plus on montre qu'il est nécessaire d'utiliser une équation précise de densité en comparant les résultats avec ceux qui utilisent une équation parabolique pour l'eau autour de 4°C.

VERTIKALE, INSTATIONÄRE, NATÜRLICHE KONVEKTION IN KALTEM WASSER

Zusammenfassung—Die instationär einsetzende Strömung infolge natürlicher Konvektion, die durch eine plötzliche Änderung der Randbedingung an einer vertikalen Oberfläche in Gang kommt, wurde untersucht. Das umgebende Medium ist kaltes Wasser, dessen Dichte sich nichtlinearisierbar mit der Temperatur ändert. Geschlossene Lösungen für die Strömungsgeschwindigkeit lassen sich aus den bekannten Lösungen für die Temperatur ermitteln. Zwei wichtige Oberflächenbedingungen wurden betrachtet: (a) Ein anfänglicher Sprung in der Oberflächenbeheizung für Oberflächen, die entweder eine unendlich kleine oder aber eine endliche Wärmekapzität besitzen; (b) Ein Sprung der Oberflächentemperatur. Die Strömungsrechungen wurden für Umgebungstemperaturen im Breich des Dichtemaximums durchgeführt. Für plötzlich beheizte Oberflächen haben Umgebungstemperaturen oberhalb des Dichemaximums für alle Zeiten eine Aufwärtsströmung zur Folge, obwohl die Geschwindigkeiten viel kleiner sind als diejenigen bei höheren Temperaturen und identischen Heizbedingungen. Für die Randbedingung (a) haben Umgebungstemperaturen unterhalb des Dichtemaximums für kleine Zeiten eine reine Abwärtsströmung zur Folge, auf die später eine nach zwei Richtungen orientierte Strömung folgt. Für die Randbedingung (b) ergeben sich durch eine passende Transformation der Geschwindigkeits- und Abstands-Variablen kongruente Verläufe. Die Bedingungen, bei denen sich eine Aufwärts-, eine nach zwei Seiten gerichtete oder eine abwärtsgerichtete Strömung ergeben, wurden untersucht. Dimensionsvergleiche der hier vorgestellten Ergebnisse mit denjenigen bei höheren Temperaturen zeigen, dass sich der Boussinesq-Ansatz in der Umgebung des Dichtemaximums nicht anwenden läßt. Zusätzlich zeigt sich—durch Vergleich der Ergebnisse mit den nach einer parabolischen Dichtebeziehung für Wasser um 4°C gewonnenen—die Notwendigkeit, eine genaue Dichtebeziehung zu verwenden.

ВЕРТИКАЛЬНЫЕ НЕУСТАНОВИВШИЕСЯ ЕСТЕСТВЕННОКОНВЕКТИВНЫЕ ТЕЧЕНИЯ В ОБЪЕМЕ ХОЛОДНОЙ ВОДЫ

Аннотация—Исследовались начальные неустановившиеся естественноконвективные течения, возникающие из-за изменения граничного условия на поверхности вертикальной пластины. Пластина помещалась в емкость с холодной водой, плотность которой нелинейно росла с температурой. Из известных решений для температуры получены решения в замкнутом виде для скорости течения. Рассматривались два важных условия на поверхности: (а) начальный скачок в подаваемой к поверхности тепловой мощности как при нулевой, так и конечной теплоемкостях поверхности и (б) скачок температуры поверхности. Скорость течения рассчитывалась для всего диапазона изменения температуры воды вблизи точки максимальной плотности. При мгновенном нагреве поверхности, когда температура окружающей воды превышала температуру максимальной плотности, возникало подъемное течение, которое не затухало длительное время, но скорость которого была однако намного ниже скорости, отмечаемой в случае более высоких значений температуры при идентичных условиях нагрева. В случае граничного условия (а) в воде с температурой, ниже температуры максимальной плотности, возникало кратковременное опускное течение, которое сменялось затем двунаправленным течением. Для условия (б) получены автомодельные профили путем соответствующего преобразования величин скорости и расстояния. Затем проводился анализ условий, при которых возникают подъемные и опускные течения, а также двунаправленное течение. Сравнение методом анализа размерностей результатов настоящего исследования с данными, полученными при более высоких значениях температуры окружающей среды, показывает непригодность приближения Буссинеска для условий вблизи точки максимальной плотности. Кроме того, из сравнения с результатами, в которых используется параболическое уравнение плотности для воды при 4 С, обоснована необходимость учета точной зависимости плотности от температуры.